Boltzmann equation and Monte Carlo analysis of electron-electron interactions on electron distributions in nonthermal cold plasmas

M. Yousfi, A. Himoudi, and A. Gaouar
Centre de Physique Atomique, Laboratoire des Decharges dans les Gaz, Université Paul Sabatier, 118 Route de Narbonne, 31 062 Toulouse CEDEX, France

(Received 10 February 1992; revised manuscript received 3 August 1992)

Electron distribution functions in nonthermal cold plasmas generated by classical electrical discharges have been calculated from a powerful Boltzmann equation solution and an original Monte Carlo simulation. In these two methods both classical (i.e., elastic, inelastic, and superelastic) electron-atom (or molecule) collisions and electron-electron interactions are taken into account. The approximations considered to include long-range (electron-electron) and short-range (electron-atom) interactions in the same Monte Carlo algorithm are first validated by comparing with Boltzmann equation results. Then, the influence of electron-electron interactions on electron distribution functions, swarm parameters, and reaction rates under nonthermal cold plasma conditions are analyzed and discussed as a function of reduced electric field E/N and ionization degree n_e/N for different atomic and molecular gases.

PACS number(s): 52.20.Fs, 51.50.+v

I. INTRODUCTION

The nonthermal cold plasmas of concern in this paper are generated by classical electrical discharges with an applied electric field E which accelerates, in particular, an electron swarm through a background gas with gas density N.

The main features of these nonthermal cold plasmas are particularly a relatively low ionization degree ($n_e/N < 10^{-4}$, n_e being electron density) and an electron temperature T_e generally higher than background gas temperature T (T is around ambient temperature). It is well known that the latter characteristic is at the origin (via electron-molecule or atom collisions) of production in the plasma of various ionized, excited, and dissociated species whose properties can then be exploited in numerous plasma devices (gas lasers, lamp discharges, plasma etching, and sputtering, flue gas treatment, etc.). Numerical modeling, which is now considered as a necessary complement to experimental investigations, can be useful to predict the optimal operating conditions of such plasma devices. Among the basic quantities required for numerical modeling, the electron distribution function is probably the most important, because electrons are responsible for most energy transfer phenomena in this kind of plasma.

The electron distribution function, which is of course far from being Maxwellian in the most typical nonthermal cold plasmas, is sensitive to numerous phenomena: electric field heating, electron source or sink, electron- molecule collisions (elastic, inelastic, and superelastic), and in certain cases electron-electron interactions.

Numerous studies based on Boltzmann equation solutions (see, for example, Ref. [1]) or on Monte Carlo simulations (see, for example, Ref. [2]) are devoted to calculation of electron distribution functions and associated transport coefficient in nonthermal cold plasmas generated by gas discharges, but without including Coulomb interaction effects. However, for certain plasmas (created, for example, in positive column of low pressure lamp discharges or in excitation medium of excimer lasers), the ionization degree becomes high enough so that the electron distribution function can be more or less affected by electron-electron interactions. Therefore it becomes necessary to include such effects on distribution function calculations in order to avoid some more or less important errors on the parameters depending directly (swarm parameters and reaction rates) or indirectly (e.g., densities of excited or ionized species, space charge distribution, etc.) on electron distribution function.

In the literature, there are also numerous studies based on Boltzmann equation solutions which already include electron-electron interaction effects on the distribution function of electrons moving under electric field action (e.g., Ref. [3]. However, in the present paper, we propose to investigate and to analyze in a systematic way the effects of electron-electron interactions on the electron distribution function and the associated transport coefficients as a function of ionization degree n_e/N, reduced electric field E/N, and also the nature of the gas (atomic or molecular) either from Boltzmann equation or Monte Carlo simulation. The method of homogeneous and time-dependent Boltzmann equation solution proposed in this paper is based on a stable and powerful numerical scheme. It is different from the classical scheme of Rockwood (used by numerous authors) since, due to the iterative nature of the present work scheme, there is no restriction for the treatment of any kind of collisions involving electrons (elastic, superelastic, inelastic, and also ionization stepwise or Penning ionization). Concerning the treatment of electron-electron interactions with the Monte Carlo method, there is a fundamental drawback due to the nonlinear nature of such interactions since the scattering depends, in particular, on the electron distribution function itself which is not known in the

beginning of the simulation. Therefore, in this paper, an original method is proposed to avoid such a drawback for the treatment of electron-molecule and electron-electron interactions with the same Monte Carlo algorithm. The first results obtained from these Monte Carlo methods including electron-electron interactions are already presented elsewhere (Yousfi *et al.* [4]). Other Monte Carlo results, for transport of electron swarm in gas discharges, are also given by Weng and Kushner [5] and Hashigushi [6] but the treatment of electron-electron interactions by the present work method is quite different especially from Hashigushi's.

Furthermore, the reader interested by the problem of the treatment of electron-electron and electron-molecule interactions with either Monte Carlo or Boltzmann equation methods can find a relatively abundant literature not only in the field of the transport of electron swarm in gas discharges [3–6], but also in other fields such as electron transport in earth's ionosphere [7] or electron transport in interstellar gas (e.g., Shull [8]) or charge transport in semiconductors (e.g., [9]) or plasmas generated by electron beam (e.g., [10]). However, in particular in aeronomy and astrophysics fields (i.e., [7] and [8]), the reader must known that the electron-electron interactions concern interactions between energetic projectile electrons and thermal target electrons whose Maxwellian distribution is already known. This is not the case in the field of our interest (i.e., electron swarm in gas discharge) where projectile and target electrons have the same unknown distribution. In any case, the problem of electron-electron interaction treatment with particularly Monte Carlo methods has not been, to the authors' knowledge, rigorously treated and still remains an interesting challenge. This is why one of the purposes of this paper is to present a Monte Carlo method based on the classical null collision technique and using successive approximations for the electron distribution function which ensure self-consistency of the solution in the presence of electron-molecule and electron-electron interactions.

The methods of Boltzmann solution and Monte Carlo simulation including both electron-atom and electron-electron collisions are described in Sec. II, while the references for collision cross sections for atomic and molecular gases used in this paper are reported in Sec. III with the corresponding results (electron distribution functions, swarm parameters, and reaction rates).

II. METHODS OF CALCULATION

A. Boltzmann equation

The usual approach considered in this paper to solve the following Boltzmann equation,

$$\frac{\partial f(\mathbf{r},\mathbf{v},t)}{\partial t}+\mathbf{v}\frac{\partial f(\mathbf{r},\mathbf{v},t)}{\partial \mathbf{r}}+\gamma\frac{\partial f(\mathbf{r},\mathbf{v},t)}{\partial \mathbf{v}}=C[f], \quad (1)$$

is based on the first term of the development of distribution function $f(\mathbf{r},\mathbf{v},t)$ in series of electron density $n_e(\mathbf{r},t)$ gradients proposed by Kumar [11]:

$$f(\mathbf{r},\mathbf{v},t)=F(\mathbf{v},t)n_e(\mathbf{r},t) . \quad (2)$$

$C[f]$ is the scattering term, $\gamma(=eE/m)$ the electric field E acceleration, and e/m the electron charge to mass ratio. $f(\mathbf{r},\mathbf{v},t)$ depends on position $\mathbf{r}$, velocity $\mathbf{v}$, and time t. The new distribution function $F(\mathbf{v},t)$ depends no longer on position $\mathbf{r}$ because development (2) is valid only when electrons are far enough from the system boundaries or electron sources and if the density gradients are small. It is then easy to obtain, from Eq. (1) and development (2), the kinetic equation verified by function $F(\mathbf{v},t)$, i.e.,

$$\frac{\partial F(\mathbf{v},t)}{\partial t}+\gamma\frac{\partial F(\mathbf{v},t)}{\partial \mathbf{v}}+\Omega(t)F(\mathbf{v},t)=C[F] , \quad (3)$$

where $\Omega(t)=[1/n_e(t)][dn_e(t)/dt]$ is the effective ionization frequency and $n_e(t)$ the electron number density.

In Eq. (3), when only binary collisions are taken into account, the scattering term $C[F]$ can be approximated by

$$C[F]=-\nu(v)F(\mathbf{v},t)+J[F] \quad (4)$$

in which $\nu(v)F(\mathbf{v},t)d\mathbf{r}d\mathbf{v}$ and $J[F]d\mathbf{r}d\mathbf{v}$ correspond to the electron number scattered, respectively, out of and into the elementary volume of phase space $d\mathbf{r}d\mathbf{v}$. In the case when the elastic, inelastic, and superelastic electron-atom and electron-electron collision processes are taken into account, the scattering term can have the following form:

$$\nu(v)=\nu_{\mathrm{el}(e\text{-}a)}(v)+\nu_{\mathrm{in}(e\text{-}a)}(v)+\nu_{\mathrm{sup}(e\text{-}a)}(v)+\nu_{\mathrm{el}(e\text{-}e)}(v) , \quad (5a)$$

$$J[F]=J_{\mathrm{el}(e\text{-}a)}[F]+J_{\mathrm{in}(e\text{-}a)}[F]+J_{\mathrm{sup}(e\text{-}a)}[F]+J_{\mathrm{el}(e\text{-}e)}[F] . \quad (5b)$$

In depopulation term $\nu(v)F(\mathbf{v},t)$, $\nu(v)$ is the total microscopic collision frequency including the elastic $\nu_{\mathrm{el}(e\text{-}a)}(v)$, inelastic $\nu_{\mathrm{in}(e\text{-}a)}(v)$, and superelastic $\nu_{\mathrm{sup}\,(e\text{-}a)}(v)$ electron-atom collisions and also electron-electron $\nu_{\mathrm{el}(e\text{-}e)}(v)$ interactions; the population term $J[F]$ involves also the same processes. Expressions of the different terms of $J[F]$ are already given elsewhere [12,13].

Kinetic equation (3) has not been directly solved under its form (3). It has been first multiplied by Legendre polynomial $P_l(\cos\theta)$ (θ is the angle between γ and $\mathbf{v}$) and integrated over $d\cos\theta$; then the classical two-term development ($l=0$ and 1) is considered. Under these conditions, Eq. (3), when collisions are assumed isotropic, becomes

$$\frac{\partial\phi_0(v,t)}{\partial t}+\frac{\gamma}{3v^2}\frac{\partial v^2\phi_1(v,t)}{\partial v}+\{\Omega(t)+\nu(v)\}\phi_0(v,t)=J[\phi_0] , \quad (6a)$$

$$\phi_1(v,t)=-\frac{1}{\Omega(t)+\nu(v)}\left[\gamma\frac{\partial\phi_0(v,t)}{\partial v}+\frac{\partial\phi_1(v,t)}{\partial t}\right] . \quad (6b)$$

$\phi_0(v,t)$ and $\phi_1(v,t)$ represent the isotropic part and first anisotropy defined as follows:

$$\phi_l(v,t)=\frac{2l+1}{2}\int_{-1}^{+1}P_l(\cos\theta)F(\mathbf{v},t)d\cos\theta .$$

In fact, $\phi_0(v,t)$ is obtained from numerical solution of the following equation deduced by setting (6b) in (6a) and developing the elastic population terms ($J_{\mathrm{el}(e\text{-}a)}[\phi_0]$ and $J_{\mathrm{el}(e\text{-}e)}[\phi_0]$):

$$v^2\frac{\partial\phi_0(v,t)}{\partial t}-\frac{\gamma^2}{3}\frac{\partial}{\partial v}\left[\frac{v^2}{\Omega(t)+\nu(v)}\frac{\partial\phi_0(v,t)}{\partial v}\right]-\frac{k_BT}{M}\frac{\partial}{\partial v}\left[v^2\nu_{\mathrm{el}(e\text{-}a)}\frac{\partial\phi_0(v,t)}{\partial v}\right]$$
$$-\frac{m}{M}\frac{\partial}{\partial v}\{v^3\nu_{\mathrm{el}(e\text{-}a)}\phi_0(v,t)\}-\frac{1}{2}\frac{\partial}{\partial v}\left[\nu_{\mathrm{el}(e\text{-}e)}v^3[A_2(v,t)+A_3(v,t)]\frac{\partial}{\partial v}\phi_0(v,t)\right]$$
$$-\frac{1}{2}\frac{\partial}{\partial v}\{\nu_{\mathrm{el}(e\text{-}e)}v^3A_1(v,t)\phi_0(v,t)\}+\{\Omega(t)+\nu(v)\}v^2\phi_0(v,t)$$
$$=v^2\{J_{\mathrm{in}(e\text{-}a)}[\phi_0]+J_{\mathrm{sup}(e\text{-}a)}[\phi_0]\}+\frac{\gamma}{3}\frac{\partial}{\partial v}\left[\frac{v^2}{\Omega(t)+\nu(v)}\frac{\partial\phi_1(v,t)}{\partial t}\right], \quad (7)$$

with the following expressions for electron-electron Coulomb terms $A_1(v,t)$, $A_2(v,t)$, and $A_3(v,t)$:

$$A_1(v,t)=\frac{4\pi}{n_e}\int_0^v\phi_0(v',t)v'^2dv' ,$$
$$A_2(v,t)=\frac{4\pi}{n_e}\frac{1}{3v}\int_0^v\phi_0(v',t)v'^4dv' , \quad (8)$$
$$A_3(v,t)=\frac{4\pi}{n_e}\frac{v^2}{3}\int_v^\infty\phi_0(v',t)v'dv'$$

and with this normalization condition: $4\pi\int_0^\infty\phi_0(v,t)v^2dv=1$. k_B represents the Boltzmann constant, T and M the temperature and mass of background gas.

Equation (7) is a time first-order and a velocity second-order partial differential equation. In this paper, the numerical scheme is chosen explicit in time and implicit in velocity. The discretization of $\partial/\partial t$ and $\partial/\partial v$ operators is made by dividing the time D_t and electron speed D_v variation domains in I and J intervals, i.e.,

$$D_v=\{0,v_{\max}\}=\{v_0=0,v_1,v_2,\ldots,v_{i-1},v_i,$$
$$v_{i+1},\ldots,v_I=v_{\max}\},$$
$$D_t=\{0,t_{\max}\}=\{t_0=0,t_1,t_2,\ldots,t_{j-l},t_j,$$
$$t_{j+1},\ldots,t_J=t_{\max}\}.$$

The left-hand side of the discretized equation thus derived depends on function $\phi_0(v,t)$ expressed only on $\phi_0(v_{i-1},t_j)$, $\phi_0(v_i,t_j)$, and $\phi_0(v_{i+1},t_j)$. When the subscript i varies from 0 to I, we obtain for every time t_j (j varying from 1 to J), a system of $I+1$ equations whose main matrix is tridiagonal. Such a system is solved with a classical numerical algorithm (Thomas algorithm), the boundary [$\phi_0(v=0,t)$ and $\phi_0(v=v_{\max},t)$] conditions, and also the initial [$\phi_0(v,t_0=0)$] condition being known. However, as the Coulomb terms $A_1(v,t)$, $A_2(v,t)$, and $A_3(v,t)$ and the effective ionization frequency $\Omega(t)$ depend on $\phi_0(v,t)$, Eq. (7) is nonlinear. The right-hand term of Eq. (7) also depends on $\phi_0(v,t)$ and $\phi_1(v,t)$. For these reasons Eq. (7) is solved by iteration. For the first step time t_1 and for the first iteration, an initial distribution is assumed for the unknown functions $\phi_0(v,t_1)$ and $\phi_1(v,t_1)$ [e.g., the known initial distributions $\phi_0(v,t_0)$ and $\phi_1(v,t_0)$]. This allows a first approximation for $\Omega(t)$, Coulomb terms, and right-hand terms of Eq. (7). The new solution $\phi_0(v,t)$ obtained is then injected in $\Omega(t)$, Coulomb terms, and right-hand terms. The same procedure is continued until the convergence of the method is reached. The functions $\phi_0(v,t)$ and $\phi_1(v,t)$ are then calculated for the next time t_j; iterations are always started from the distribution functions at time t_{j-1}. It is important to note that for every time step and also for every iteration, $\phi_0(v,t)$ is obtained from solution of Eq. (7) following the numerical procedure described above and $\phi_1(v,t)$ is then obtained from Eq. (6b). The fact that $\phi_1(v,t)$ in Eq. (6b) depends on itself via a time derivative term $[\partial\phi_1(v,t)/\partial t]$ is absolutely not a problem because, as the numerical method is iterative, $\phi_1(v,t)$ is also obtained by successive approximations simultaneously with $\phi_0(v,t)$. In the literature the time derivative term $\partial\phi_1(v,t)/\partial t$ of Eq. (6b) is usually neglected (see, for example, Winkler, Wilhelm, and Hess [14]). Such approximation, which is certainly correct when the steady-state solution is reached, could be completely incorrect during the transient phase of the evolution of electron swarm [15].

B. Monte Carlo simulation

1. *Treatment of electron-molecule collisions*

The electron transport in a gas under the influence of an electric field E can be simulated with the help of a Monte Carlo method from an initially great number of seed electrons. These primary electrons are followed one by one until their disappearance out of the domain of the simulation. Every electron, during its transit in the gas, performs a succession of free flights punctuated by elastic or inelastic or superelastic collisions with molecules (or atoms) of gas defined by collision cross sections. During the successive collisions for every electron, a certain quantity of information (velocity, position, etc.) are stored in order to calculate, from appropriate sampling methods, distribution function, swarm parameters, and

reaction rates. The simulation is stopped when all the primary electrons as well as the secondary electrons (created, for example, by ionization) are treated.

The Monte Carlo algorithm used in this paper is a classical one (see, for example, Reid [2]). Between two successive collisions the free time of flight, the electron trajectory, the collision type, and the electron velocity before and after every collision must be known.

Time between two successive collisions or (time of free flight) t_{flight} is calculated, by using the null collision method initially developed by Skullerud [16] for simulation of ion motion in gases:

$$t_{\text{flight}} = -\frac{\ln(r_{\text{flight}})}{\nu_{\text{tot}}} , \tag{9}$$

where r_{flight} is a random number uniformly distributed in the [0,1] range and ν_{tot} is the total collision frequency including the total electron-molecule collision frequency $\nu_{e\text{-}a}$ and a null collision frequency ν_{null} chosen in order to always have ν_{tot} constant:

$$\nu_{\text{tot}} = \nu_{e\text{-}a} + \nu_{\text{null}} = \text{const} .$$

While the trajectory between two successive collisions is obtained from the classical mechanics equations, i.e., from the electric field strength $\mathbf{F}$ exercised on electrons with a charge $-e$: $\mathbf{F} = -e\mathbf{E} = m d\mathbf{v}/dt = m d^2\mathbf{r}/dt^2$. In the laboratory Cartesian system of coordinates and in the case of an electric field $\mathbf{E}$ antiparallel to the Oz axis, this relation becomes

$$\frac{dv_x}{dt} = \frac{d^2x}{dt^2} = 0 , \quad \frac{dv_y}{dt} = \frac{d^2y}{dt^2} = 0 , \quad \frac{dv_z}{dt} = \frac{d^2z}{dt^2} = \frac{eE_z}{m} . \tag{10}$$

Hence, starting from a velocity $\mathbf{v}_0(v_{x0}, v_{y0}, v_{z0})$ at time t_0 corresponding either to initial velocity of primary electron or to velocity just after the last collision (at the beginning of free flight), the component of electron velocity $\mathbf{v}_1$ (v_{x1}, v_{y1}, v_{z1}) at time t_1 just before the next collision (i.e., at the end of the free flight) is obtained by integrating relations (10) over time range $[t_0, t_1]$ where $t_{\text{flight}} = t_1 - t_0$, i.e.,

$$v_{x1} = v_{x0} , \quad v_{y1} = v_{y0} , \quad v_{z1} = v_{z0} + \frac{eE_z}{m} t_{\text{flight}} . \tag{11}$$

On the other hand, the new coordinates $\mathbf{r}_1(x_1, y_1, z_1)$ of an electron at time t_1 can be calculated from coordinates $\mathbf{r}_0(x_0, y_0, z_0)$ of an electron at time t_0 by integrating relations (11), i.e.,

$$\begin{aligned} x_1 &= x_0 + v_{x0} t_{\text{flight}} , \quad y_1 = y_0 + v_{x0} t_{\text{flight}} , \\ z_1 &= z_0 + v_{z0} t_{\text{flight}} + \frac{1}{2} \frac{eE_z}{m} t_{\text{flight}}^2 . \end{aligned} \tag{12}$$

Starting from the electron parameters $\mathbf{r}_0, \mathbf{v}_0, t_0$ at the beginning of the free flight, the new electron parameters $\mathbf{r}_1, \mathbf{v}_1, t_1$ at the end of the free flight are obtained, respectively, from relations (12), (11), and (9). Then just after the collision occurring at time t_1, the electron parameters become $\mathbf{r}_1'$, $\mathbf{v}_1'$, t_1'. However, it is necessary to calculate only electron velocity $\mathbf{v}_1'$ because the electron-molecule interaction is assumed instantaneous ($t_1' = t_1$) and local ($\mathbf{r}_1' = \mathbf{r}_1$). Velocity $\mathbf{v}_1'$ is calculated from knowledge of the collision type which is given by the likelihoods ($p_{\text{col,el}}$, $p_{\text{col,in}}$, $p_{\text{col,sup}}$ or $p_{\text{col,null}}$) of occurrence of every collision kind (elastic, inelastic, superelastic, or null):

$$p_{\text{col,el}} = \frac{\nu_{\text{el}(e\text{-}a)}}{\nu_{\text{tot}}} , \quad P_{\text{col,in}} = \frac{\nu_{\text{in}(e\text{-}a)}}{\nu_{\text{tot}}} ,$$

$$p_{\text{col,sup}} = \frac{\nu_{\text{sup}(e\text{-}a)}}{\nu_{\text{tot}}} , \quad p_{\text{col,null}} = \frac{\nu_{\text{null}}}{\nu_{\text{tot}}} ,$$

with $p_{\text{col,el}} + p_{\text{col,in}} + p_{\text{col,sup}} + p_{\text{col,null}} = 1$.

The type of collision is then determined from a random number r_{col} uniformly distributed between 0 and 1. Several types of collision are possible: (1) if it is a null collision, velocities before and after the collision are the same, (2) if it is, e.g., an attachment, the next primary electron is treated, and (3) if it is another real collision, the velocity $\mathbf{v}_1'$ after interaction depends on the collision type; the component of electron velocity $\mathbf{v}_1'$ as a function of $\mathbf{v}_0$ and $\mathbf{v}_1$ is given in the Appendix for the different collision types.

2. *Treatment of electron-electron and electron-molecule interactions*

There are essentially two major drawbacks to treating electron-molecule and electron-electron interactions with the same Monte Carlo algorithm.

The first one is linked to the nature of interaction itself. Electron-molecule interactions are short-range interactions: they can then be approximated as binary collisions and treated with laws of classical mechanics, whereas electron-electron interactions are long-range interactions: this means every projectile electron can interact simultaneously (multiple interactions) with numerous target electrons situated inside its Debye sphere, because interactions with charged particles outside the Debye sphere (collective effects) are negligible in usual nonthermal cold plasmas ($n_e/N < 10^{-4}$).

The second drawback is linked to the distribution of target particles. In the case of electron-molecule collisions, the distribution of molecular target is known (Maxwellian at gas temperature), whereas in the case of electron-electron interactions, the distribution of electronic target is unfortunately unknown; the latter's distribution is exactly the same distribution as for the projectile electrons and is therefore the distribution sought.

In order to avoid the first drawback, the multiple electron-electron interactions are first assumed as a succession of binary collisions weakly deviated: this corresponds to the classical Fokker-Planck approximation already taken into account for Coulomb scattering terms in Boltzmann equation [see relations (8)]. Under this approximation, Coulomb interactions can be treated as binary collisions, but there is still the problem of multiple collisions (i.e., a simultaneous great number of collisions). A supplementary assumption is therefore necessary to include electron-electron interactions in the Monte Carlo algorithm with reasonable time computing. This second

assumption consists of grouping every succession of weak deflection binary collisions into a unique binary collision with a larger scattering angle integrating the contribution of all the weak scattering angles. In practice, this means the projectile electron undergoes a binary elastic collision with a fictitious target electron having the same mean energy as the target electrons situated inside its Debye sphere; such a fictitious electron therefore keeps all its characteristics from an energetic point of view.

In order to avoid the drawback of the unknown electron target distribution, for the first primary electrons treated, a known electron target distribution is assumed (e.g., a Maxwellian distribution). When the following primary electrons are treated, the mean distribution of the previous electrons is considered: for example, for the ith primary electron, the mean distribution of the $(i-1)$th previous primary electrons is considered. As the number of treated primary electrons increases, the distribution of target electrons is progressively improved: for the results given in Sec. III in N_2 discharge for $E/N=10$ Td, the statistic fluctuations become very acceptable from 3000 primary electrons on.

Thus the previous approximations allow us to consider electron-electron interactions as simple binary collisions which can therefore be treated with the Monte Carlo algorithm already described in Sec. II B 1. However, the determination of the free time of flight t_{flight} and also the collision type necessitates taking into account the supplementary electron-electron process. t_{flight} becomes

$$t_{\text{flight}}=-\frac{\ln(r_{\text{flight}})}{\nu_{\text{tot}}} \quad \text{with } \nu_{\text{tot}}=\nu_{e\text{-}a}+\nu_{e\text{-}e}+\nu_{\text{null}}=\text{const} .$$

Electron-electron collision frequency $\nu_{e\text{-}e}$ has the following form:

$$\nu_{e-e}=\frac{n_e}{N}N\int v_r\sigma_{e\text{-}e}(v_r)F(\mathbf{r},\mathbf{v}_t,t)d\mathbf{v}_t . \tag{13}$$

v_r is the relative speed ($\mathbf{v}_r=\mathbf{v}-\mathbf{v}_t$), $\mathbf{v}_t$ is the velocity of the fictitious target electron, and $\mathbf{v}$ is, as previously defined, the projectile electron velocity [in the $\nu_{e\text{-}e}$ relation, the distribution function $F(\mathbf{r},\mathbf{v}_t,t)$ of target electrons is normalized to unit and $\sigma_{e\text{-}e}(v_r)$ is the Coulomb cross section].

The determination of the collision type also requires the calculation of collision likelihood $p_{\text{col},e\text{-}e}$ of electron-electron interactions: $p_{\text{col},e\text{-}e}=\nu_{e\text{-}e}/\nu_{\text{tot}}$, with

$$p_{\text{col,el}}+p_{\text{col,in}}+p_{\text{col,sup}}+p_{\text{col,null}}+p_{\text{col},e\text{-}e}=1 .$$

Furthermore, it is important to note that null collision frequency ν_{null} must be chosen high enough in order to have total collision frequency ν_{tot} which always verifies this inequality: $\nu_{\text{tot}}>\nu_{e\text{-}a}+\nu_{e\text{-}e}$. Such caution is necessary because $\nu_{e\text{-}e}$, which depends on the electron distribution function [see relation (13)], is not known *a priori* (i.e., in the beginning of Monte Carlo simulation) contrarily to $\nu_{e\text{-}a}$. This is the reason for which ν_{null} must be overestimated to be sure that $\nu_{\text{tot}}>\nu_{e\text{-}a}+\nu_{e\text{-}e}$, particularly at lower values of electron speed where $\nu_{e\text{-}e}$ is maximum.

III. BASIC DATA AND RESULTS

A. Collision cross sections

In the following some results are given for different atomic and molecular gases in order to emphasize the specific behavior of each gas when the influence of electron-electron processes becomes significant. References of elastic and inelastic (excitation and ionization) electron-atom collision cross sections for the different rare gases (He, Ne, Ar, Kr, and Xe) have already been given by Yousfi *et al.* [13] while collision cross sections for the molecular gas chosen (N_2) come from Phelps and Pitchford [17]. Figure 1 shows, as an illustration, momentum transfer cross sections for the different gases analyzed in this paper. The electron-electron elastic cross section used is the classical one (see, e.g., Rockwood [3]).

B. Results and discussion

The aim of this section is mainly to analyze and to discuss the influence of electron-electron interactions on electron distribution functions, swarm parameters, and reaction rates as a function of ionization degree n_e/N, reduced electric field E/N, and also the gas. But first, in order to validate Monte Carlo treatment of electron-electron interactions as is considered in Sec. II B 2, some comparisons between Monte Carlo and Boltzmann equation results are presented.

1. Comparisons between Monte Carlo and Boltzmann equation results

Figure 2 shows the isotropic part of the electron distribution 1 function in N_2 for $E/N=10$ Td with and without considering electron-electron interactions. Monte Carlo and Boltzmann equation distribution functions are comparable in the entire energy range (distribution bulk and tail). However, if in Monte Carlo simulation the energy distribution of target electrons is assumed Maxwellian (such as Hashigushi [6]), there are deviations,

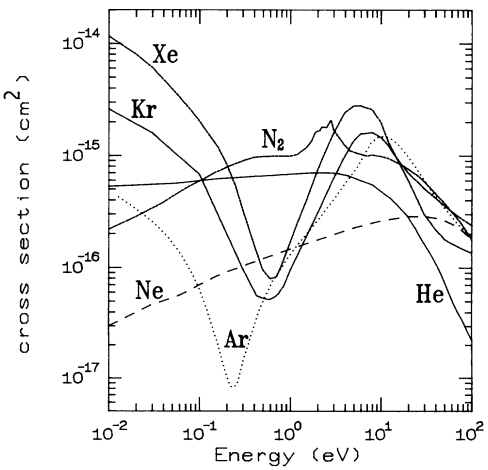

FIG. 1. Elastic momentum transfer cross section in rare gases (He, Ne, Ar, Kr, and Xe) and in N_2.

particularly in distribution bulk above mean energy value of the Maxwellian distribution chosen (i.e., around 0.8 eV). These deviations vanish as soon as the distribution function is calculated following the Monte Carlo algorithm described in Sec. II B 2, i.e., the distribution of target electrons is progressively approximated by the distribution of projectile electrons. Furthermore, the good agreement observed concerning distribution functions is, as expected, completely carried over to swarm parameters (drift velocity or mean energy) plotted in Fig. 3 as a function of time. Noting the classical transient phase before reaching equilibrium state and noting also the shortness of relaxation time of mean energy and drift velocity as n_e/N increases: it is due to the rising of total collision frequency (inversely proportional to relaxation time) consecutive to the electron-electron frequency rising. Other

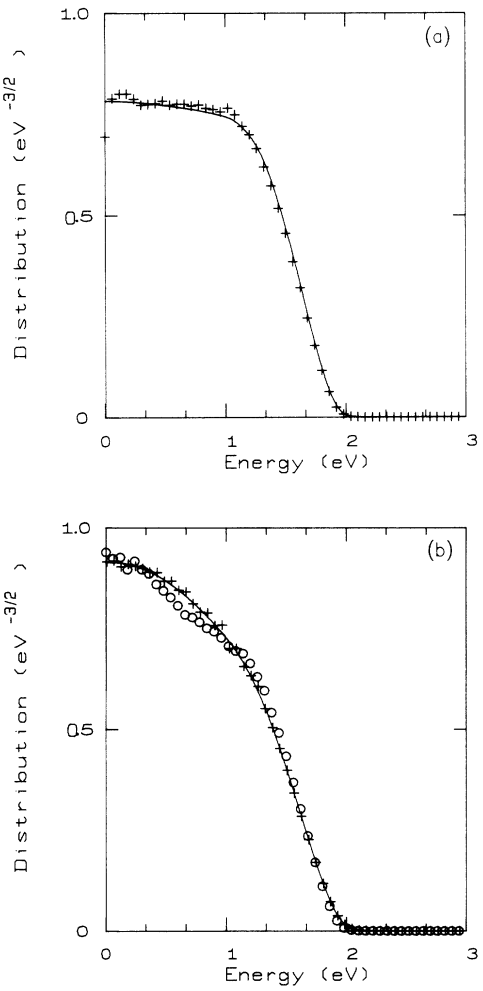

FIG. 2. (a) Isotropic part of electron distribution function in N_2 for $E/N=10$ Td without electron-electron interactions: $++$, Monte Carlo simulation; ——, Boltzmann equation solution. (b) Isotropic part of electron distribution function in N_2 for $E/N=10$ Td with electron-electron interactions ($n_e/N=10^{-5}$): ——, Boltzmann equation solution; Monte Carlo simulation with a Maxwellian distribution for target electrons (○○) and with the same distribution for target and incident electrons ($++$).

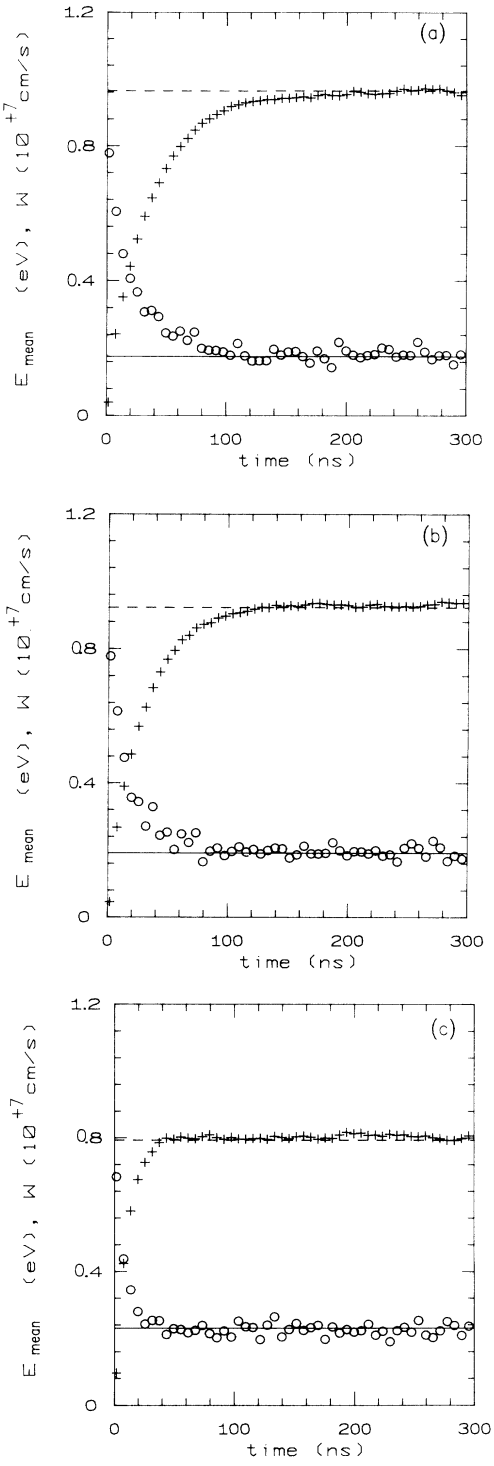

FIG. 3. (a) Electron mean energy ($++$, $---$) and drift velocity (○○, ——) in N_2 for $E/N=10$ Td without electron-electron interactions. Symbols: Monte Carlo simulation; lines: Boltzmann equation solution. (b) Electron mean energy ($++$, $---$) and drift velocity (○○, ——) in N_2 for $E/N=10$ Td with electron-electron interactions ($n_e/N=10^{-5}$). Symbols: Monte Carlo simulation; lines: Boltzmann equation solution. (c) Electron mean energy ($++$, $---$) and drift velocity (○○, ——) in N_2 for $E/N=10$ Td with electron-electron interactions ($n_e/N=10^{-4}$). Symbols: Monte Carlo simulation; lines: Boltzmann equation solution.

results obtained for other E/N values and in other gases but not reported in this paper confirm the good agreement observed in Figs. 2 and 3. This means approximations chosen in this paper to include electron-electron interactions in the Monte Carlo algorithm are reasonably good for the case of usual nonthermal cold plasma ($n_e/N < 10^{-4}$).

2. *Electron-electron interaction effects on distribution functions*

In a first overview of Fig. 2, the influence of electron-electron interactions on the isotropic part of the distribution function can already be noted. It can be observed that the low-energy part of the distribution is enhanced as n_e/N increases, showing the presence of a greater electron number in this low-energy region. But this is not the only effect of Coulomb interactions on distribution functions.

Figures 4(a), 4(b), and 4(c) show the isotropic part of the distribution function in different gases (Ne, Ar, and N_2) without and with electron-electron interactions for several ionization degrees ($n_e/N = 10^{-6}$, 10^{-5}, and 10^{-4}) and for a relatively low E/N value ($E/N = 5$ Td). These gases are chosen for the specific behavior of electrons on each of them. For instance, dominant collision processes at 5 Td are elastic collisions in Ne, also elastic collisions in Ar but with a peculiar shape for elastic cross section (Ramsauer minimum: see Fig. 1) and inelastic (mainly vibrational excitation at low E/N), superelastic, and to a lesser degree elastic collisions in N_2. The specific shape of the distribution tail in N_2 observed in Fig. 4(c) is due to a conjunction of electron-electron interactions and superelastic collisions. Despite the differences observed, as expected, on the localization in energy axis of the distribution bulk and tail for each gas, because, in particular, electron mean energy is not the same, the isotropic part shows similar behavior as n_e/N increases (i.e., when the Coulomb interaction effect becomes stronger). In fact, if the energy scale is divided in three regions: low-energy region (region 1), intermediate-energy region or distribution bulk (region 2), and high-energy region or distribution tail (region 3), this similar behavior can be analyzed as follows. As n_e/N increases, the isotropic part in regions 1 and 3 is enhanced, while in region 2 it is lowered; this effect is much more accentuated for higher n_e/N values. In other words, the isotropic part shrinks towards Maxwellian distribution, which is a straight line in a semilogarithmic plot, as n_e/N increases. The limit is reached when n_e/N nears 1 (quasi-ionized gas): in that case the electron distribution nears, of course as it is already known, a completely Maxwellian distribution. In order to explain such an effect (i.e., Maxwellianization of distribution function under the influence of electron-electron interactions), which is not always sufficiently explained in the literature, Fig. 5 shows a schematic representation of the three previous energy regions, the isotropic part of the distribution function (with and without electron-electron interactions) and also the electron-electron collision frequency $\nu_{e\text{-}e}(\varepsilon)$ as a function of kinetic energy. The reasons for which the distribution func-

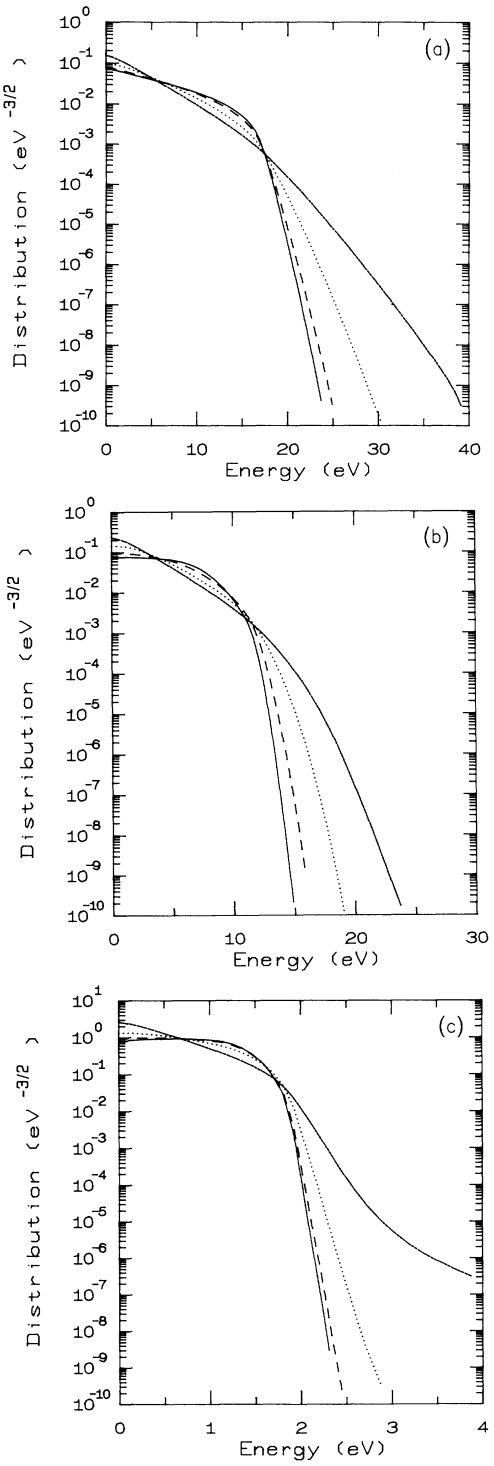

FIG. 4. (a) Isotropic part of electron distribution function in Ne for $E/N = 5$ Td without (——), and with electron-electron interactions (dashed lines): — — —, $n_e/N = 10^{-6}$; · · ·, $n_e/N = 10^{-5}$; and –··–, $n_E/N = 10^{-4}$. (b) Isotropic part of electron distribution function in Ar for $E/N = 5$ Td without (——) and with electron-electron interactions (dashed lines): — — —, $n_e/N = 10^{-6}$; · · ·, $n_e/N = 10^{-5}$; and –··–, $n_e/N = 10^{-4}$. (c) Isotropic part of electron distribution function in N_2 for $E/N = 5$ Td without (——) and with electron-electron interactions (dashed lines): — — —, $n_e/N = 10^{-6}$; · · ·, $n_e/N = 10^{-5}$; and –··–, $n_e/N = 10^{-4}$.

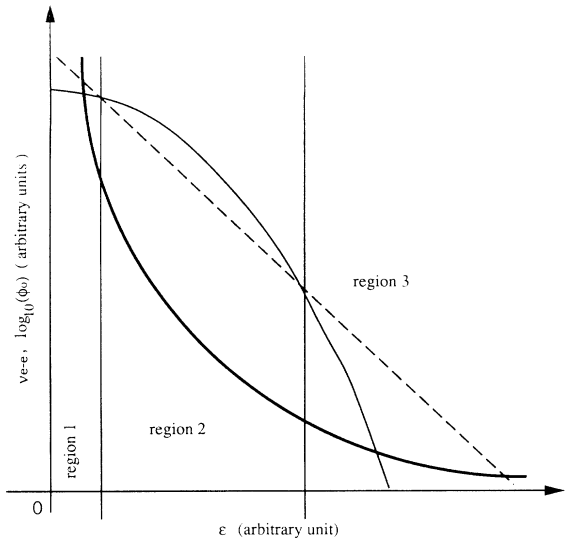

FIG. 5. Schematic representation of electron-electron interaction frequency $\nu_{e\text{-}e}$ (——), isotropic part of distribution function ϕ_0 without (——), and with (— — —) electron-electron interactions, and the three (low-, intermediate-, and high-) energy regions.

tion is lowered in region 2 to the detriment of energy regions 1 and 3 under the effect of electron-electron interactions are given hereafter. If an electron from region 2 undergoes an electron-electron interaction, it can be, for instance, ejected in region 1 (i.e., energy loss), at the same time another electron is automatically ejected towards region 3 (energy gain) since electron-electron interactions do not change the total energy of electron gas. Therefore, if electron-electron interactions occurring in region 2 are important enough [which is not always the case because $\nu_{e\text{-}e}(\varepsilon)$ rapidly decreases in region 2: see Fig. 5], this can explain, following the energy conservation principle, the rise of ϕ_0 function in regions 1 and 3 to the detriment of region 2.

The schematic representation in Fig. 5 corresponds to a relatively low E/N value. For higher E/N values, the distribution function—but not $\nu_{e\text{-}e}(\varepsilon)$—is shifted towards high-energy regions. This means the relative importance of $\nu_{e\text{-}e}(\varepsilon)$ diminishes particularly in regions 2 and 3. And as E/N becomes too high, the magnitude of $\nu_{e\text{-}e}(\varepsilon)$ can become completely negligible in regions 2 and 3. Consequently, the distribution function is practically not affected by electron-electron interactions for high E/N values. Such a behavior is confirmed in Figs. 6(a), 6(b), and 6(c) showing the isotropic part ϕ_0 of the distribution function plotted with and without electron-electron interactions for increasing E/N values (1, 10, and 50 Td) in Ne, Ar, and N_2. The decreasing effect of electron-electron interactions with increasing E/N values is quite spectacular in particular for distribution tail in Ne and Ar. However, in N_2, due in particular to the high magnitude of inelastic processes (excitation of vibrational and certain optical levels), electrons are slowed down and concentrated in relatively low-energy regions (lower than around 5 eV) and therefore distribution tail is not very sensitive to electron-electron interactions for high E/N in N_2.

3. *Electron-electron interaction effect on swarm parameters*

Following results of Figs. 4 and 6, the decreasing influence of electron-electron interaction on distribution function is clearly emphasized as E/N increases. The problem is to know from what E/N value this influence becomes negligible, knowing that such a limit depends on gas and also n_e/N. This can be analyzed from swarm parameters (e.g., drift velocity W) and reaction rates (e.g., ionization frequency ν_{ion}), as they are representative, respectively, of distribution bulk and tail behavior.

Figures 7 and 8 show reduced ionization frequency ν_{ion}/N and drift velocity W calculated without and with inclusion of electron-electron interactions for several n_e/N values in the case of Ne, Ar, and N_2.

First of all, at low E/N values the increasing of ν_{ion}/N, due to electron-electron interactions, observed in Figs. 7(a) and 7(b) is more pronounced for higher n_e/N (10^{-4}). This can be explained by the rising distribution tail observed in Fig. 4 which, as is known, directly influences ν_{ion}/N magnitude. However, ν_{ion}/N in N_2 is practically insensitive to electron-electron interactions whatever n_e/N [see Fig. 7(c)], for the reasons already evoked in the preceding section concerning the distribution tail in N_2 which is not very sensitive to electron-electron interactions.

However, the effect of electron-electron interactions on drift velocity W is completely different because W is representative not only of the distribution tail as ν_{ion}/N but also and mainly of the distribution bulk. In Figs. 8(a), 8(b), and 8(c), W behaves similarly whatever the gas (Ne, Ar, or N_2) depending on the E/N range considered. In fact, three different E/N ranges can be distinguished: the first one (range 1) corresponds to the very low E/N values where drift velocities calculated without W_w and with $W_{e\text{-}e}$ including electron-electron interactions verify this inequality: $W_w > W_{e\text{-}e}$. In the second E/N range (range 2), this order is inverted ($W_w < W_{e\text{-}e}$) and in the last range (range 3) the electron-electron interaction effect becomes negligible ($W_w \cong W_{e\text{-}e}$). Of course, boundaries of each E/N range depend on gas and n_e/N (see Fig. 8); for instance, range 2 varies, for $n_e/N = 10^{-4}$, from around 1 up to 130 Td in N_2 and from around 0.3 up to 40 Td in Ne. Drift velocity behavior in each E/N range can be explained as follows. Range 1 corresponds to a situation where the distribution function is affected by electron-electron processes essentially at very low energy (energy region 1 previously defined). In this energy region where the distribution function is reinforced, as is shown in Figs. 3–5, total elastic momentum transfer collision frequency (for electron-electron and also electron-atom interactions) increases with n_e/N. Then, electron distribution becomes more isotropic, which diminishes drift velocity, because W is in a certain way a measure of the anisotropy of electron swarm in the gas. This can be better quantified from the classical relation obtained by Phelps [1] from the Boltzmann equation:

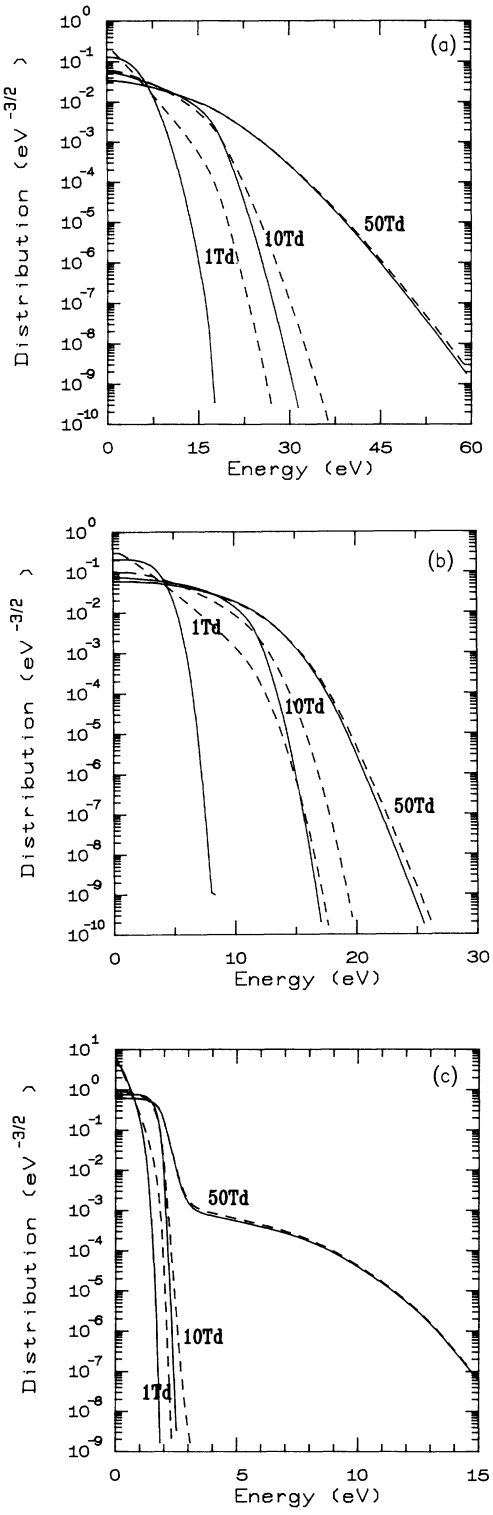

FIG. 6. (a) Isotropic part of electron distribution function in Ne without (——) and with (— — —) electron-electron interactions for $n_e/N=10^{-5}$, and $E/N=1$, 10, and 50 Td. (b) Isotropic part of electron distribution function in Ar without (——) and with (— — —) electron-electron interactions for $n_e/N=10^{-5}$, and $E/N=1$, 10, and 50 Td. (c) Isotropic part of electron distribution function in N_2 without (——) and with (— — —) electron-electron interactions for $n_e/N=10^{-5}$, and $E/N=1$, 10, and 50 Td.

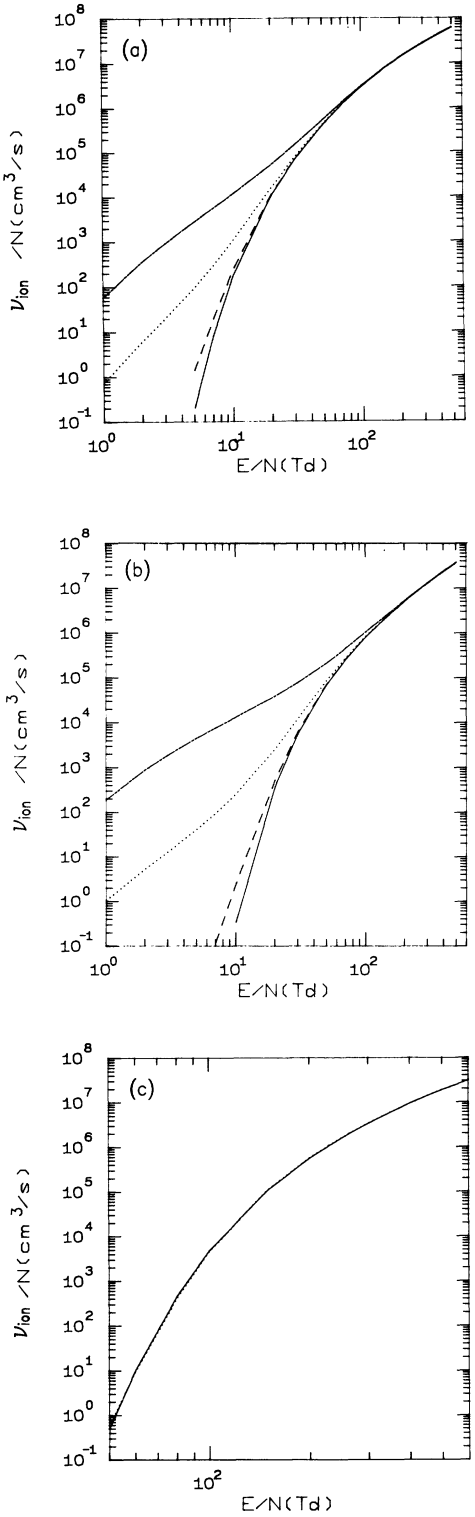

FIG. 7. (a) Ionization frequency in Ne without (——) and with (dashed lines) electron-electron interactions: — — —, $n_e/N=10^{-6}$; · · ·, $n_e/N=10^{-5}$; and –··–, $n_e/N=10^{-4}$. (b) Ionization frequency in Ar without (——), and with (dashed lines) electron-electron interactions: — — —, $n_e/N=10^{-6}$; · · ·, $n_e/N=10^{-5}$; and –··–, $n_e/N=10^{-4}$. (c) Ionization frequency in N_2 without (——), and with (dashed lines) electron-electron interactions: — — —, $n_e/N=10^{-6}$; · · ·, $n_e/N=10^{-5}$; and –··–, $n_e/N=10^{-4}$.

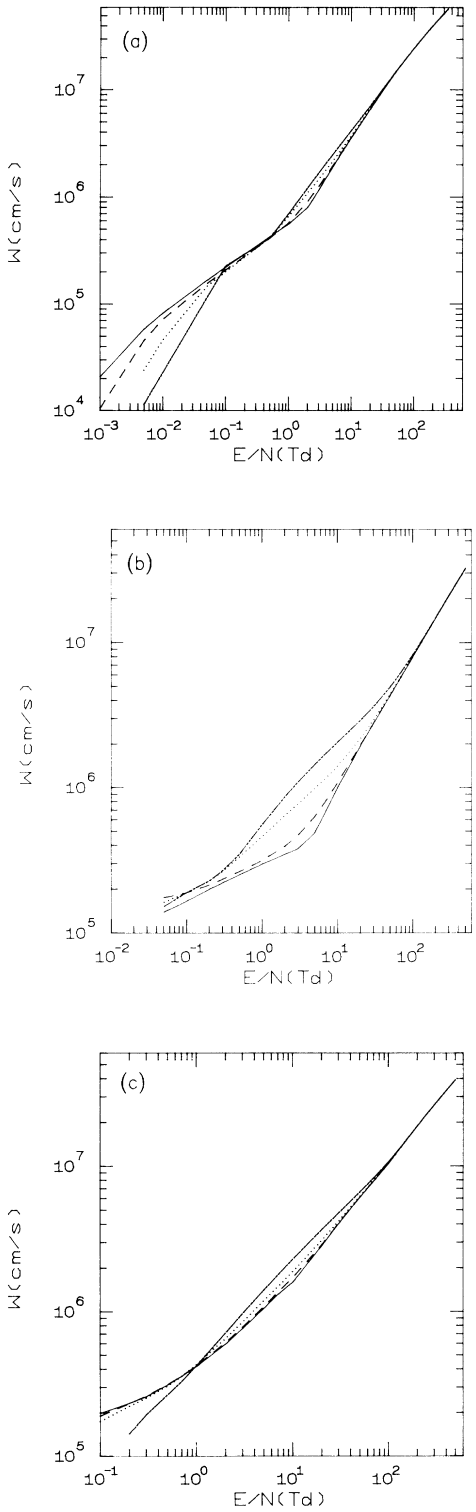

FIG. 8. (a) Electron drift velocity in Ne without (——), and with (dashed lines) electron-electron interactions: — — —, $n_e/N=10^{-6}$; · · ·, $n_e/N=10^{-5}$; and –··–, $n_e/N=10^{-4}$. (b) Electron drift velocity in Ar without (——), and with (dashed lines) electron-electron interactions: — — —, $n_e/N=10^{-6}$; · · ·, $n_e/N=10^{-5}$; and –··–, $n_e/N=10^{-4}$. (c) Electron drift velocity in N_2 without (——), and with (dashed lines) electron-electron interactions: — — —, $n_e/N=10^{-6}$; · · ·, $n_e/N=10^{-5}$; and –··–, $n_e/N=10^{-4}$.

$W=(eE/m)1/\langle\nu_m\rangle$, where W is inversely proportional to the macroscopic momentum transfer collision frequency $\langle\nu_m\rangle$. Another proportionality relation (Phelps [1]) useful to better understand drift velocity behavior particularly in range 2 (intermediate E/N values) is $W=\langle\nu_{in}\rangle[(D/\mu-kT/e)/E]$, where D/μ is the energy characteristic and $\langle\nu_{in}\rangle$ the macroscopic inelastic collision frequency. In range 2, as n_e/N increases, the inelastic processes represented by $\langle\nu_{in}\rangle$ are reinforced because distribution tail is enhanced. Therefore W increases following the previous proportion relation between W and $\langle\nu_{in}\rangle$.

The growth of inelastic processes for higher n_e/N values is clearly illustrated in Figs. 9(a) and 9(b) from the energy loss per elastic, excitation, and ionization collisions as a function of E/N in, for instance, Ar. At low E/N values, when electron-electron interactions are not taken into account, most of the electron energy is lost by

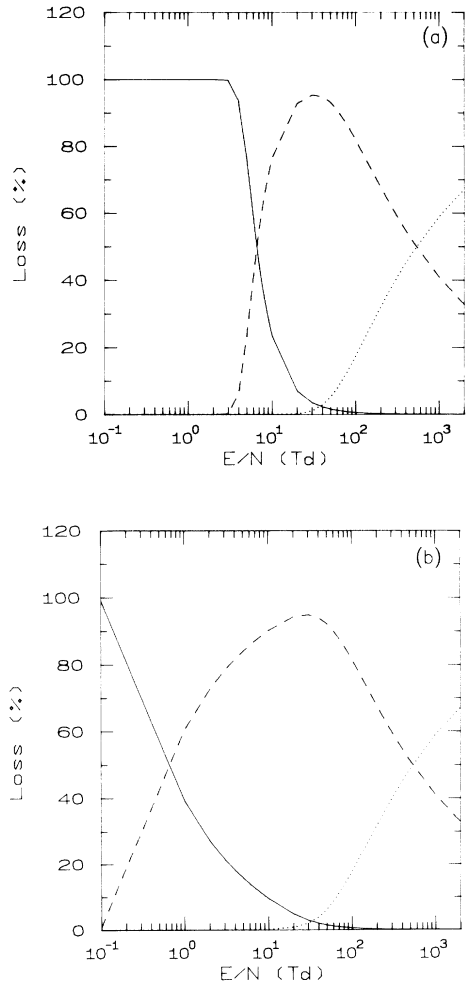

FIG. 9. (a) Percentage of energy losses in Ar by elastic (——), excitation (— — —), and ionization (· · ·) electron-atom collisions without electron-electron interactions. (b) Percentage of energy losses in Ar by elastic (——), excitation (— — —), and ionization (· · ·) electron-atom collisions with electron-electron interactions for $n_e/N=10^{-5}$.

elastic collisions until around 3 Td [Fig. 9(a)]. However, as soon as electron-electron interactions are considered, it is easy to observe in Fig. 9(b) that energy lost by elastic collisions begins to decrease for lower E/N values (<0.1 Td) to the detriment of energy lost by inelastic processes (excitation and then ionization collisions). This behavior corresponds totally to the rise of distribution tail in the presence of electron-electron interactions already emphasized in this section.

Finally, whatever the gas or n_e/N value, the effect of electron-electron interactions on drift velocity or ionization frequency becomes negligible from a limiting E/N value (E/N_{lim}) which is different according to the macroscopic parameter considered (W or ν_{ion}/N). This limiting value E/N_{lim} is given, as an example, in Table I for $n_e/N=10^{-4}$, knowing that electron-electron effect is considered negligible if the relative difference between the macroscopic parameter with and without electron-electron interactions is lower than 5%. We note that, concerning ν_{ion}/N for N_2, there is no E/N lim because ionization frequencies with and without electron-electron interactions are not different whatever E/N [see also comment concerning Fig. 7(c)].

The last figures show electron drift velocity calculated in Xe for two quite low E/N values (1 and 10 Td) as a function of ionization degree [Fig. 10(a)] and the relative difference $\Delta W/W$ between drift velocity calculated with and without electron-electron interactions [Fig. 10(b)]. $\Delta W/W$ is lower than 5% for $n_e/N<10^{-7}$ but $\Delta W/W$ increases rapidly with n_e/N; for example, in Xe and for $n_e/N=10^{-5}$, $\Delta W/W$ can reach around 60% for 1 Td. Such drastic differences on swarm parameters show, if necessary, the important role played by electron-electron interactions on electron kinetics under discharge parameters (n_e/N, E/N, gas, etc.) usual for formation of nonthermal cold plasmas. Of course the typical nonthermal cold plasmas where electron-electron interactions are usually not negligible (e.g., excitation medium for excimer lasers) are formed under more complex conditions (gas mixtures, time dependence of E/N and n_e/N, etc.) and electron kinetics is also perturbed by other collisional processes (e.g., heavy particle collisions). However, the results obtained in this paper concerning the relative importance of electron-electron interactions on the distribution function and swarm parameters remains valid at least qualitatively for these more complex plasmas, because electron-electron interactions concern interactions between electrons themselves.

TABLE I. Limiting E/N value for drift velocity $E/N_{\text{lim},W}$ and for ionization frequency $E/N_{\text{lim},\nu_{\text{ion}}}$ with $n_e/N=10^{-4}$.

Gas	$E/N_{\text{lim},W}$ (Td)	$E/N_{\text{lim},\nu_{\text{ion}}}$ (Td)
Helium	10	50
Neon	40	80
Argon	120	150
Krypton	150	190
Xenon	160	200
Nitrogen	130	5

ACKNOWLEDGMENT

The authors would like to acknowledge A. Alkaa since a part of this paper was elaborated in the framework of his work [19]. The Laboratoire des Decharges dans les Gaz is "Unité de Recherche associée au CNRS No. 277."

APPENDIX: KINEMATICS OF COLLISIONS

Once the type of real collision has been determined, it is necessary to calculate electron velocity $\mathbf{v}_1'$ just after the collision. In the collision system, vector $\mathbf{v}_1'$ can be defined in spherical coordinates by electron speed v_1', scattering angle χ and azimuthal angle η.

(a) Scattering angle χ, between velocity $\mathbf{v}_1$ before and $\mathbf{v}_1'$ after the collision, varies between 0 and π; χ depends on differential cross section $\sigma(v,\chi)$. It is determined from a uniform random number r_χ belonging to the [0,1] range:

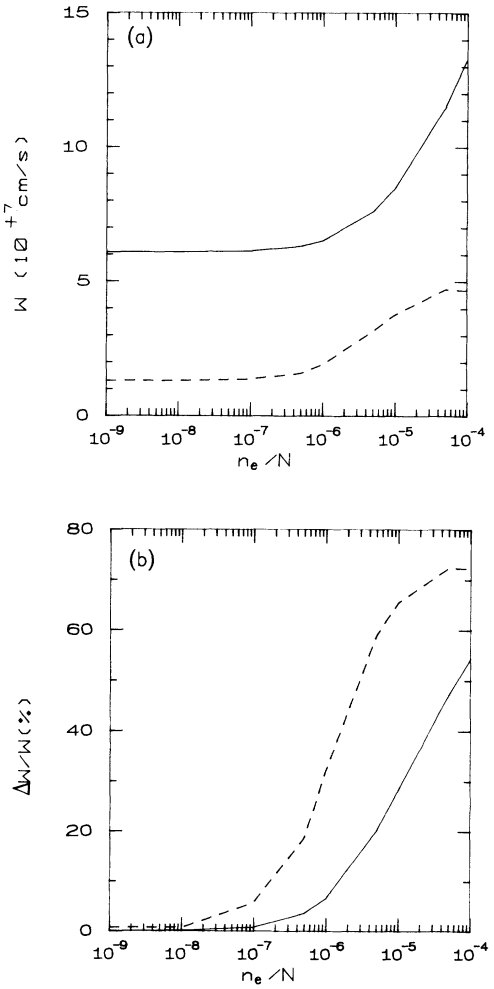

FIG. 10. (a) Electron drift velocity in Xe as a function of ionization degree for $E/N=1$(— — —) and 10 Td (——). (b) Relative difference on electron drift velocity in Xe calculated with and without electron-electron interactions as a function of ionization degree for $E/N=1$(— — —) and 10 Td (——).

$$r_\chi = \frac{\int_0^\chi \sigma(v,\chi)\sin\chi' d\chi'}{\int_0^\pi \sigma(v,\chi)\sin\chi' d\chi'} ;$$

if an isotropic scattering is assumed this relation becomes $\cos\chi = 1 - 2r_\chi$.

(b) Azimuthal angle η is assumed in this paper to be uniformly distributed in the $[0,2\pi]$ range; it is then calculated from a uniform random number r_η belonging to the [0,1] range, i.e., $\eta = 2\pi r_\eta$.

(c) Electron speed v_1' just after the collision depends of course on the type of collision which has occurred. In the case of an elastic collision, due to the low value of electron-molecule ratio m/M and since the target molecule is considered to be at rest, the electron speed (or energy) after the elastic collision is given by

$$\tfrac{1}{2}mv_1'^2 = \tfrac{1}{2}mv_1^2 \left[1 - 2\frac{m}{M}(1-\cos\chi) \right] .$$

In the case of inelastic collision corresponding to the excitation energy threshold ε_{ex} and since the energy recoil of the molecule can be assumed negligible in comparison to ε_{ex}, the electron speed (or energy) is approximated by the relation $\frac{1}{2}mv_1'^2 = \frac{1}{2}mv_1^2 - \varepsilon_{ex}$. In the case of superelastic collision corresponding, for instance, to deexcitation processes from energy level ε_{ex} to ground state, the previous relation becomes $\frac{1}{2}v_1'^2 = \frac{1}{2}mv_1^2 + \varepsilon_{ex}$. In the case of a simple ionization process with threshold ε_{ion}, the residual energy just after collision is shared between scattered (ε_{sc}) and ejected (ε_{ej}) electrons following the approximated relation $\varepsilon_{sc} + \varepsilon_{ej} = \frac{1}{2}mv_1^2 - \varepsilon_{ion}$. The energy sharing depends on the knowledge of differential ionization cross section $\sigma_{ion}(\varepsilon_1,\varepsilon)$. For example, the energy of ejected electron ε_{ej} can be obtained from a uniform random number r_{ion} belonging to the [0,1] range:

$$r_{ion} = \frac{\int_0^{\varepsilon_{ej}} \sigma_{ion}(\varepsilon_1,\varepsilon)d\varepsilon}{\sigma_{ion}(\varepsilon_1)} ,$$

where $\sigma_{ion}(\varepsilon_1)$ is the integral ionization cross section and ε_1 the incident energy ($\frac{1}{2}mv_1^2$). For electron swarm moving through a gas under electric field action, the influence of electron-electron interactions is not negligible only for low E/N where ionization processes do not play an important role. Therefore, concerning differential cross section $\sigma_{ion}(\varepsilon_1,\varepsilon)$, it is possible to assume, with a relatively good approximation for low E/N values, that the residual ionization energy is equally shared between ejected and scattered electrons, i.e., $\varepsilon_{ej} = r_{ion}(\varepsilon_1 - \varepsilon_{ion})/2$. However, in order to have a correct energy distribution after ionization, it is better to use differential cross-section data available in the literature (e.g., [18]). In this case, a consequent inconvenience is that Monte Carlo calculations become computationally more time consuming. Concerning deflection angles of scattered and ejected electrons after the ionizing collision, it can be assumed that the scattered electron is deviated following the χ angle and the ejected electron following χ' with $\chi' = \chi + \pi/2$.

Once the $\mathbf{v}_1'$ components (i.e., v_1', χ, and η) are known in the collision system, it is then necessary to determine them in the laboratory system. The Cartesian components of vector $\mathbf{v}_1'$ can be written in laboratory system as a function of polar θ_1 and azimuthal ϕ_1 angles of incident vector $\mathbf{v}_1$ by using the classical Euler transformation relations:

$$v_{x1}' = v_1'\{ \sin\chi\cos\eta\sin\phi_1 + \sin\chi\sin\eta\cos\theta_1\cos\phi_1 + \cos\chi\sin\eta\cos\phi_1 \} ,$$

$$v_{y1}' = v_1'\{ -\sin\chi\cos\eta\cos\phi_1 + \sin\chi\sin\eta\cos\theta_1\sin\phi_1 + \cos\chi\sin\eta\sin\phi_1 \} ,$$

$$v_{z1}' = v_1'\{ -\sin\chi\sin\eta\sin\phi_1 + \cos\chi\cos\theta_1 \} .$$

Finally, in the case of an elastic collision between two particles without neglecting the velocity (or the energy) recoil of the target particle, the previous relations are no longer valid. Kinematics of such a collision need to be reconsidered. Assume two particles of masses m and M, velocities $\mathbf{v}_1$ and $\mathbf{V}_1$ before elastic collision and $\mathbf{v}_1'$ and $\mathbf{V}_1'$ after the collision. Unknown velocities $\mathbf{v}_1'$ and $\mathbf{V}_1'$ are obtained from the classical conservation equations of momentum transfer and energy and also from knowledge of scattering χ and azimuthal η angles of vector $\mathbf{v}_1'$ in the collision system. So, components of $\mathbf{v}_1'$ and $\mathbf{V}_1'$ in the laboratory system are then determined from

$$\mathbf{v}_1' = \frac{M}{m+M} v_r \mathbf{u} + \frac{m\mathbf{v}_1 + M\mathbf{V}_1}{m+M} ,$$

$$\mathbf{V}_1' = -\frac{m}{m+M} v_r \mathbf{u} + \frac{m\mathbf{v}_1 + M\mathbf{V}_1}{m+M} ,$$

where v_r is the relative speed ($\mathbf{v}_r = \mathbf{v}_1 - \mathbf{V}_1$) and $\mathbf{u}$ the unit vector directed along $\mathbf{v}_1'$. Such relations are useful in the case of very low E/N value where thermal motion of molecular target gas cannot be neglected in comparison to electron incident energy and, also in the case of Coulomb interaction treatment in the framework of approximations considered in Sec. II B 2 corresponding to impact between a projectile electron and a fictitious target electron.

[1] A. V. Phelps, Rev. Mod. Phys. **40**, 399 (1968); Y. Sakai, H. Tagashira, and S. Sakamoto, J. Phys. D **10**, 1051 (1977); S.L. Lin, R. E. Robson, and E. A. Mason, J. Chem. Phys. **71**, 3483 (1979).

[2] T. Itoh and T. Musha, J. Phys. Soc. Jpn. **15**, 1675 (1960); A. I. Mc Intosh, Aust. J. Phys. **27**, 59 (1974); I. D. Reid, *ibid.* **32**, 231 (1979).

[3] S. D. Rockwood, Phys. Rev. A **8**, 2348 (1973); J. Appl. Phys. **45**, 5229 (1974); R. B. Winkler, J. Wilhelm, and R. Winkler, Ann. Phys. (N. Y.) **40**, 90 (1983); W. Dezhen and M. Tengeai, J. Phys. D **24**, 1367 (1991); J. A. Kunc and W. H. Soon, Phys. Rev. A **43**, 4409 (1991).

[4] M. Yousfi, A. Alkaa, O. Lamrous, and A. Himoudi, in *Proceedings of the 2nd Congrès de la Division Plasma de la Société Française de Physique, C15, Université Paris–Sud, Orsay, 1990;* in *Proceedings of the 43rd Annual Gaseous Electronic Conference, University of Illinois, Urbana-Champaign, 1990,* p. 155.
[5] Y. Weng and M. J. Kushner, Phys. Rev. A **42**, 6192 (1990).
[6] S. Hashigushi, IEEE Trans. Plasma Sci. **19**, 297 (1991).
[7] M. H. Rees, *Physics and Chemistry of the Upper Atmosphere* (Cambridge University Press, Cambridge, England, 1988); E. Oran and D. J. Strickland, Planet. Space Sci. **26**, 1161 (1978); R. J. Cicerone and S. A. Bowhill, J. Geophys. Res. **76**, 8299 (1971).
[8] J. M. Shull, Astrophys. J. **234**, 761 (1979).
[9] A. Matulionis, J. Pozela, and A. Reiklaitis, Solid State Commun. **16**, 1133 (1975); J. Bacchelli and C. Jacobini, *ibid.* **10**, 71 (1977).
[10] C. J. Elliott and A. E. Green, J. Appl. Phys. **47**, 2946 (1976); J. Bretagne, J. Godart, and V. Puech, J. Phys. D 15, 2205 (1982).
[11] K. Kumar, J. Phys. D **14**, 2199 (1981).
[12] M. Yousfi and A. Chatwiti, J. Phys. D **20**, 457 (1987).
[13] M. Yousfi, G. Zissis, A. Alkaa, and J. J. Damelincourt, Phys. Rev. A **42**, 978 (1990).
[14] R. Winkler, J. Wilhelm, and A. Hess, Ann. Phys. (N. Y.) **7**, 537 (1985).
[15] M. Yousfi, A. Gaouar, O. Lamrous, and J. Fassi, in *Proceedings of the Tenth International Conference on Gas Discharges and their Applications, Swansea, 1992,* edited by W. T. Williams, pp. 840–843.
[16] H. R. Skullerud, J. Phys. D **1**, 1567 (1968).
[17] A. V. Phelps and L. C. Pitchford, JILA Information Center Report No. 26, 1985 (unpublished).
[18] C. B. Opal, W. K. Peterson, and E. C. Beaty, J. Chem. Phys. **55**, 4100 (1971).
[19] A. Alkaa, Ph.D. thesis No. 967, Université Paul Sabatier, Toulouse, 1991 (unpublished).